

Fidelity of the acoustic control of single photon scattering with semiconductor quantum dots

RAFAŁ A. BOGACZEWICZ AND PAWEŁ MACHNIKOWSKI*

Institute of Theoretical Physics, Wrocław University of Science and Technology, 50-370 Wrocław, Poland

**pawel.machnikowski@pwr.edu.pl*

Compiled October 11, 2024

Acoustic modulation of quantum dots (QDs) allows one to control the scattering of photons. Here we theoretically characterize the fidelity of acoustic control of the scattering in the frequency domain. We formulate the theory of low-intensity resonance fluorescence in the presence of white noise and show that a high degree of control is achievable with a two-tone acoustic field for appropriate settings of modulation amplitudes as long as the noise-induced phase diffusion coefficient remains one order of magnitude smaller than the acoustic frequency. In addition, using a quantitative model of optical signal collection, we determine that the acoustic phase must be stable over 10^4 to 10^5 acoustic periods for efficient control.

<http://dx.doi.org/10.1364/ao.XX.XXXXXX>

1. INTRODUCTION

In recent years, resonant light scattering (resonance fluorescence, RF) has found many applications in solid-state systems, such as entangling single photons with quantum dot (QD) spins [1], reading out quantum information encoded in solid-state qubits [2, 3] and generating indistinguishable photons [4]. Acoustic modulation of a quantum emitter offers additional control of the light scattering process. In the resolved sideband regime, where the acoustic frequency is larger than the line width [5, 6], the RF spectrum of a weakly optically excited and acoustically modulated QD contains the usual central line, located at the laser frequency [7], and a series of sidebands induced by modulation, which correspond to phonon emission and absorption at the quantum level [8, 9]. The scattered photons are antibunched [6, 10], indicating the single-photon nature of the scattering.

Acoustic wave mixing has been shown to provide precise control over the scattering of photons to a particular frequency channel [10], as well as in the time domain [11]. Two-tone acoustic driving leads to quantum interference of different pathways contributing to a given scattering process involving exchange of acoustic quanta from the two acoustic harmonics in various combinations. The quantum phase relation between the pathways is governed by the relative phase between the two acoustic waves, which allows one to control the probability of photon scattering to a given frequency sideband as a function of this phase [10].

Theoretical description has been extended to quantum acoustic modes [8], where light scattering was shown to perform a measurement of the phonon state in the Fock basis [9]. This opens up a perspective for the implementation of frequency- and time-bin encoding [12, 13], quantum multiplexing [14], quantum acousto-optic transduction [15], and other promising solutions in the field of quantum information processing. Short wavelengths of acoustic waves in the GHz (μeV) frequency (energy) range make them perfect candidates for miniaturized devices that may lay the ground for on-chip acousto-optic quantum hybrid systems [16, 17].

Whether this acoustic control can be exploited in quantum applications depends, to a large extent, on the resilience of the observed coherent acousto-optic features against external perturbations, such as charge noise due to nearby defects in a semiconductor environment [18] that cause fluctuations in the local electric field [19]. In addition, in view of the finite time required to collect the optical signal originating from a single quantum emitter, phase stability of the control fields becomes crucial.

In this paper, we present a theoretical analysis of the achievable degree of control of photon scattering by coherent acoustic modulation of a QD. We develop a model of low-excitation resonance fluorescence of a periodically modulated two-level system in the presence of white noise. This allows us to determine the scattering spectrum and to show that the relative contrast of phase-dependent intensity oscillations at the optimal setting of modulation parameters is weakly affected by noise as long as the strength of the latter remains well below the acoustic frequency. Finally, we set the minimum requirements for the stability of the acoustic frequency in these coherent acousto-optic processes.

2. MODEL

We consider a self-assembled semiconductor QD resonantly driven by a weak, monochromatic laser field. The QD transition energy is modulated acoustically by a surface acoustic wave acting via crystal strain and deformation potential coupling and is also subject to random environmental noise. The scattered photons are collected and their time-integrated spectrum is determined [10].

We model the QD as a two-level system with energy eigenstates $|0\rangle$ and $|1\rangle$ and transition energy $\hbar\omega_0(t)$, where the time dependence results from SAW modulation and environmental noise,

$$\omega_0(t) = \bar{\omega}_0 + \Delta\omega_{\text{ac}}(t) + \Delta\omega_{\text{ns}}(t), \quad (1)$$

where $\bar{\omega}_0$ is the unperturbed transition energy, whereas $\Delta\omega_{ac}(t)$ and $\Delta\omega_{ns}(t)$ denote acoustic modulation and noise contributions, respectively, both assumed to have zero average. We assume that $\Delta\omega_{ac}(t)$ is periodic with fundamental frequency ω_A . In addition, the system undergoes spontaneous emission with the rate γ .

The model is formally equivalent to that proposed in [10, 11], except that the modulation of the transition energy now contains a random component. The evolution is found by iteratively solving the Lindblad equation for the density matrix up to the second order in Rabi frequency. The detector response is described by the autocorrelation function $G(t_1, t_2) = \langle \sigma_+(t_1)\sigma_-(t_2) \rangle$, which is calculated from the system evolution using the quantum Lax regression theorem [11, 20]. In the leading order in the field amplitude (Ω^2) it reads for $t_2 > t_1$ [10]

$$G(t_1, t_2) = \frac{\Omega^2}{4} \int_{-\infty}^{\infty} du e^{-\left(\frac{\gamma}{2} + i\bar{\Delta}\right)u} e^{-i\Phi_{ac}(t_1, t_1 - u)} \quad (2)$$

$$\times \int_{-\infty}^{\infty} du' e^{-\left(\frac{\gamma}{2} - i\bar{\Delta}\right)u'} e^{i\Phi_{ac}(t_2, t_2 - u')} \mathcal{D}(u, u', t_2 - t_1),$$

where $\Phi_{ac}(t_2, t_1) = \int_{t_1}^{t_2} \Delta\omega_{ac}(s) ds$ is the deterministic contribution to the accumulated phase, $\bar{\Delta} = \omega_L - \bar{\omega}_0$, with ω_L denoting the laser frequency, and

$$\mathcal{D}(u, u', \tau) = \overline{e^{i\Phi_{ns}(0, -u) - i\Phi_{ns}(\tau, \tau - u')}} \theta(u)\theta(u') \quad (3)$$

encodes the complete information about the noise, which is assumed stationary, with $\Phi_{ns}(t_2, t_1) = \int_{t_1}^{t_2} \Delta\omega_{ns}(s) ds$, $\theta(u)$ denoting the Heaviside step function and the bar representing averaging over noise realizations. Note that $\Phi_{ac}(t_2, t_1)$ is periodic in both arguments.

We consider the simplest case of white noise that leads to phase diffusion described by a Gaussian distribution for $\Phi_{ns}(t_2, t_1)$ with variance $2D(t_2 - t_1)$, $t_2 > t_1$, where D is the phase diffusion coefficient related to the noise strength, $\langle \omega_{ns}(t)\omega_{ns}(t + \tau) \rangle = 2D\delta(\tau)$. Then we obtain for $\tau > 0$ (see Supplement 1)

$$D(u, u', \tau) = \mathcal{D}_{el}(u, u', \tau) + \mathcal{D}_{inel}(u, u', \tau),$$

where

$$\mathcal{D}_{el}(u, u', \tau) = e^{-D(u+u')\tau} \theta(u)\theta(u') \quad (4)$$

and

$$\mathcal{D}_{inel}(u, u', \tau) = e^{-D\tau} \theta(u)\theta(u' - \tau) \quad (5)$$

$$\times \left[e^{-D|u+\tau-u'|} - e^{-D(u+u'-\tau)} \right].$$

The first of the two contributions does not depend on τ , resulting in a periodic autocorrelation function that leads to a series of unbroadened spectral features. We refer to this contribution as elastic. The other contribution is damped in τ , leading to broadened spectral lines, corresponding to noise-induced inelastic scattering. This contribution vanishes as $D \rightarrow 0$.

Substituting Eq. (4) and Eq. (5) to Eq. (2) one gets the corresponding elastic and inelastic contributions to the autocorrelation function. A function periodic in its two arguments is also periodic in their sum and difference. We can therefore define functions $\phi_n(u)$ through the expansion

$$e^{i\Phi_{ac}(t-u', t-u)} = \sum_n \phi_n(u-u') e^{in\omega_A \left(t - \frac{u+u'}{2}\right)}. \quad (6)$$

For the elastic term, we then immediately find

$$G_{el}(t_1, t_2) = \frac{\Omega^2}{\gamma^2} \sum_{nm} c_n c_m^* e^{i\omega_A(nt_1 - mt_2)}, \quad t_2 > t_1, \quad (7)$$

where

$$c_n = \frac{\gamma}{2} \int_0^\infty du e^{-(\gamma/2 + D + i\bar{\Delta})u} e^{-in\omega_A u/2} \phi_n(u). \quad (8)$$

The inelastic part can be written in the form (see Supplement 1)

$$G_{inel}(t_1, t_2) = \frac{\Omega^2}{2\gamma^2} e^{-\left(\gamma/2 + D - i\bar{\Delta}\right)(t_2 - t_1)} \quad (9)$$

$$\times \sum_{nmk} b_m^* b_n b_{-k} d_k e^{i\omega_A(nt_1 - mt_2)}, \quad t_2 > t_1,$$

where b_n are the coefficients of the Fourier expansion

$$e^{-i\Phi_{ac}(t_2, t_1)} = \sum_{nm} b_m^* b_n e^{i\omega_A(nt_1 - mt_2)} \quad (10)$$

and

$$d_n = \frac{2D\gamma}{(\gamma + D + in\omega_A)^2 - D^2} (c_n + c_{-n}^*). \quad (11)$$

Both components of the autocorrelation function, as functions of τ , are sums of purely exponential contributions. Consequently, the time-integrated RF spectrum,

$$S(\omega) = \text{Re} \int_0^\infty d\tau e^{i(\omega - \omega_L)\tau} e^{-\Gamma\tau} \bar{G}(\tau), \quad (12)$$

where

$$\bar{G}(\tau) = \frac{\omega_A}{2\pi} \int_0^{2\pi/\omega_A} dt G(t, t + \tau), \quad (13)$$

has an elastic and inelastic part, both composed of a series of Lorentzians (explicit formulas are given in Supplement 1). The former is only broadened by the finite instrumental resolution Γ which we have included in the model. The spectral features of the latter are not only broadened by $\gamma/2 + D$ but also shifted by $\bar{\Delta}$, that is, from the spectral position related to the laser frequency to that bound to the unperturbed transition energy.

3. RESULTS

In this section, we first discuss the RF spectrum under monochromatic acoustic modulation in the presence of noise. Then we analyze the fidelity of acoustic control in the presence of noise. Finally, we investigate the role of acoustic phase stability.

We set $\gamma/\omega_A = 2\Gamma/\omega_A = 0.1$. RF spectra will be presented in natural units set by the maximum value of the spectrum for an unperturbed system without modulation under weak resonant excitation $S_0 = \Omega^2/(\gamma^2\Gamma)$ [7]. Similarly, the natural unit for the intensity is $I_0 = \pi\Omega^2/\gamma^2$, corresponding to the standard RF of an unperturbed weakly excited two-level system.

A. RF spectrum under harmonic modulation and noise

Substituting Eq. (7) and Eq. (9) to Eq. (13) and Eq. (12) one finds the spectrum in the form of a sum of Lorentzian contributions as well as dispersive terms in the inelastic component. We start with the case of harmonic modulation $\Delta\omega_{ac}(t) = A\omega_A \cos(\omega_A t)$. Then

$$b_n^{(1)} = J_n(A), \quad \phi_n^{(1)}(u) = i^n J_n [2A \sin(\omega_A u/2)], \quad (14)$$

where J_n is the Bessel function of the first kind. From this, the coefficients c_n and d_n can be calculated numerically using Eq. (8) and Eq. (11), respectively.

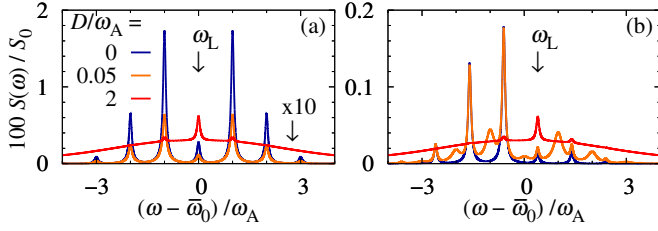


Fig. 1. RF spectrum for acoustically modulated QD with noise. Results for a single-SAW mode in case of (a) resonant excitation and for (b) $\omega_L = \bar{\omega}_0 + 0.4\omega_A$.

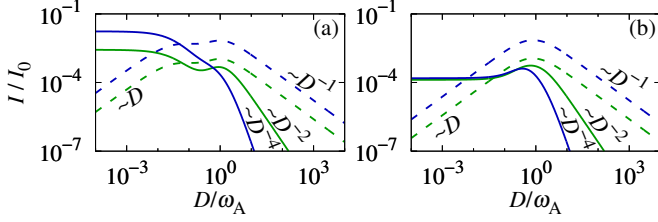


Fig. 2. Intensities of lines from elastic/inelastic series (solid/dashed lines) for $p = q = 0$ (green lines) and $p = q = 1$ (blue lines). (a) Resonant excitation; (b) $\omega_L = \bar{\omega}_0 + 0.4\omega_A$.

Fig. 1 presents the RF spectra in this case for resonant (Fig. 1a) and slightly detuned (Fig. 1b) excitation for $A = 2$. In the absence of noise (blue lines), the spectrum consists of a series of lines separated from the laser frequency by an integer multiple of ω_A [10, 11]. Upon including noise (orange and red lines), the intensities of these peaks change. In addition, an inelastic contribution appears at integer multiples of ω_A from the unperturbed transition frequency, similar to the case without modulation [20], where an inelastic peak appeared at the transition frequency. This is particularly well visible in Fig. 1b, where the laser is detuned by a fraction of acoustic frequency and the two line series appear at different frequencies. A similar inelastic contribution appears in a quantum regime, where the spectral jitter is modeled as pure dephasing [9]. While the elastic lines remain narrow, the width of the inelastic ones grows, as discussed in Sec. 2 until, for a sufficiently strong noise, they merge into a broad feature that dominates the spectrum (red lines; this regime has been reached only in Fig. 1b).

The intensity of an elastic line located at $\omega = \omega_L + p\omega_A$ is

$$I_{\text{el}}^{(p)} = I_0 |c_p|^2, \quad (15)$$

while the intensity of an inelastic contribution at $\omega = \bar{\omega}_0 + q\omega_A$ is

$$I_{\text{inel}}^{(q)} = I_0 \text{Re} b_q^* \sum_k b_{q-k} d_k / 2. \quad (16)$$

Note that the latter can be interpreted as a line intensity only when $D \ll \omega_A$; otherwise the lines lose their identity. The intensities of selected contributions are shown as functions of the phase diffusion coefficient D in Fig. 2, where the green lines correspond to the central line at resonant excitation, while blue lines represent the intensities of the first sideband of the laser frequency and transition frequency for the elastic and inelastic contributions, respectively. Figs. 2a,b correspond to the excitation conditions of Figs. 1a,b, respectively. One can see that the intensities have a power-law asymptotic dependence on D . In the limit of vanishing noise, the intensities of the elastic lines

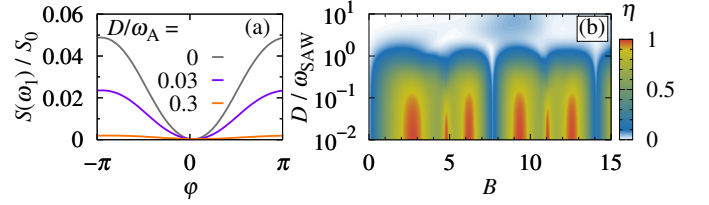


Fig. 3. (a): The scattering intensity at the spectral position of the first acoustic sideband for different noise strengths upon modulation with two commensurate harmonic acoustic waves, as a function of the relative phase between these acoustic harmonics. (b) The contrast of the phase dependence as a function of the amplitude B and the noise strength D . Here the QD is excited resonantly, $A = 1$ and $B = 2.76$ in (a).

(solid lines in Fig. 2) reach a finite value, corresponding to the $D \rightarrow 0$ limit of c_n . In this limit the intensities of the inelastic lines vanish proportionally to D , as follows from Eq. (11), restoring the purely elastic scattering of the noise-free regime [10]. For strong noise ($D \gg \gamma, \omega_A, \bar{\Delta}$), all the intensities decrease with D . From Eq. (8) one finds $c_n \sim D^{-(n+1)}$ (see Supplement 1), hence $I_{\text{el}}^{(p)} \sim D^{-2(n+1)}$. On the other hand, $d_k \sim D^{-(k+1)}$ and b_n are independent of D , hence the sum in Eq. (9) is dominated by the term containing d_0 and $I_{\text{inel}}^{(q)} \sim D^{-1}$ for each q ; therefore inelastic scattering dominates in the strong noise limit.

B. Two-tone acoustic control of photon scattering

In this section, we study the RF spectra in the presence of the acoustic modulation composed of two harmonics,

$$\Delta\omega_{\text{ac}}(t) = A\omega_A \cos(\omega_A t) + B\omega_A \cos(2\omega_A t + \varphi). \quad (17)$$

In the case of such a two-tone modulation one finds

$$b_n^{(2)} = \sum_k J_{n-2k}(A) J_k(B/2) e^{ik\varphi}, \quad (18)$$

$$\phi_n^{(2)}(u) = \sum_k i^{n-k} J_{n-2k} \left(2A \sin \frac{\omega_A u}{2} \right) J_k(B \sin \omega_A u) e^{ik\varphi}. \quad (19)$$

We will focus on the first acoustic sideband at $\omega = \omega_L + \omega_A$ under resonant excitation ($\omega_L = \bar{\omega}_0$). We will determine the scattering intensity $S(\omega_L + \omega_A)$, which corresponds directly to the number of detector counts for the spectral filter set at the first sideband.

We calculate the coefficients b_n and c_n numerically and obtain the spectrum from Eq. (12). The amplitude of the first sideband as a function of the relative phase φ is presented in Fig. 3a for different noise strengths D . Clearly, noise reduces the amplitude of phase-dependent oscillations of the scattering intensity, which is related to the overall intensity reduction discussed above.

As an intensity-independent figure of merit characterizing the fidelity of control of the scattering intensity we use the normalized contrast $\eta = (S_{\text{max}} - S_{\text{min}}) / (S_{\text{max}} + S_{\text{min}})$, where S_{max} and S_{min} are the maximum and minimum scattering intensities as a function of the phase φ . This is shown in Fig. 3b as a function of the amplitude B and the noise strength D . The contrast approaches unity when the intensity for a certain phase is close to zero. Whether this happens depends on the interplay of various Fourier components in Eq. (19). In general, for the intensity to reach zero, at least two of these components must be of comparable order, which occurs at certain values of B , corresponding to the red areas in Fig. 3(b). The striking apparent periodicity

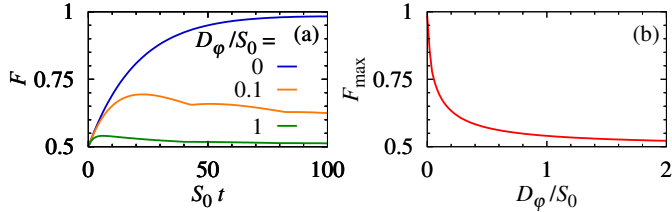


Fig. 4. Impact of the acoustic phase instability on the degree of control of the phonon scattering at $B = 2.76$: (a) The degree (fidelity) of the phase control as a function of the integration time. (b) Maximum achievable control fidelity.

of this picture as a function of B follows from the oscillating character of Bessel functions at large values of their argument. The direct dependence on $J_k(B/2)$ is explicit in Eq. (18), while in Eq. (19) it can be shown by appropriately transforming the formula (see Supplement 1). The detrimental effect of noise is stronger whenever high relative contrast is due to a very low value of S_{\min} , which makes it more vulnerable to the raising inelastic background.

Finally, we discuss the importance of the phase stability of the acoustic modulation for the efficient control of photon scattering. The optical signal from a single quantum emitter has to be integrated over a finite time to obtain meaningful results, and phase instability on this time scale affects the degree of the acoustic phase control of the scattering. As a figure of merit that captures both the accumulation of the physical signal in time and the phase perturbation, we propose the fidelity of control F , which quantifies the amount of phase information encoded in scattered photons: The phase is randomly set to the value that yields the maximum or minimum scattering rate to the first sideband. This setting is to be determined on the basis of the number of photons scattered during a time period t at the frequency of the first sideband. The fidelity F is equal to the probability of correctly determining the phase setting, with the value of $1/2$ corresponding to the null information (random guessing). The formal details are discussed in Supplement 1. For simplicity, in this discussion we assume that the background noise is absent.

In a perfectly phase-stable setup, the fidelity increases as the signal is integrated in time, asymptotically reaching the value of the contrast η (blue line in Fig. 4(a)). With phase instability, which we model as a phase diffusion with the diffusion constant D_ϕ , the phase information initially grows as photons are collected but then starts to decay since the phase diffusion blurs the initial phase setting, suppressing the difference in the corresponding scattering rates (orange and green lines in Fig. 4(a)). As a result, the maximum achievable fidelity of phase control decays very fast (see Fig. 4(b)). To give a rough estimate of the absolute numbers, $\Omega \sim 0.1\gamma$ to ensure weak coupling limit and $\Gamma \sim 0.1\omega_A$ to select the desired sideband. From Fig. 4(b) one can see that the D_ϕ must be 1–2 orders lower than $S_0 = \Omega^2/(\gamma^2\Gamma)$ for fidelities close to 1. Therefore, $D_\phi \lesssim 10^{-4}\omega_A$, that is, the acoustic phase must be stable over times 4–5 orders of magnitude longer than the acoustic period (assuming a perfect detector), which highlights the importance of the extremely high stability demonstrated in Ref. [10].

4. CONCLUSION

We have developed the theory of light scattering on a single quantum emitter with periodically modulated transition energy

in the presence of external noise and phase instability of the modulation. By applying this theory to a semiconductor QD modulated by an acoustic field composed of two harmonics and subject to external white noise, we have shown that the achievable degree of acoustic control of the photon scattering in the spectral domain remains very high for appropriate settings of the modulation amplitudes and for noise amplitudes leading to phase diffusion coefficients well below the acoustic modulation frequency. We have also highlighted the importance of the acoustic phase stability over times four to five orders of magnitude longer than the modulation period.

Our results set the limits and requirements for controlling single-photon scattering by classical acoustic waves. In a longer perspective, they may offer a starting point for the analysis of quantum information transfer from mechanical to optical qubits in frequency-bin encoding.

Funding. This work has been supported by the National Science Centre, Poland (NCN) under Grant No. 2023/50/A/ST3/00511 and by the Alexander von Humboldt Foundation under a Research Group Linkage Grant.

Acknowledgments. The authors thank Daniel Groll, Tilmann Kuhn, and Daniel Wigger for fruitful discussions.

Disclosures. The authors declare no conflicts of interest.

Data availability statement. No data were generated or analyzed in the presented research.

Supplemental document. See Supplement 1 for supporting content.

REFERENCES

1. Y. L. Delley, M. Kroner, S. Faelt, *et al.*, “Deterministic entanglement between a propagating photon and a singlet-triplet qubit in an optically active quantum dot molecule”, *Phys. Rev. B* **96**, 241410 (2017).
2. A. Muller, E. B. Flagg, P. Bianucci, *et al.*, “Resonance Fluorescence from a Coherently Driven Semiconductor Quantum Dot in a Cavity”, *Phys. Rev. Lett.* **99**, 187402 (2007).
3. G. Wrigge, I. Gerhardt, J. Hwang, *et al.*, “Efficient coupling of photons to a single molecule and the observation of its resonance fluorescence”, *Nat. Phys.* **4**, 60 (2008).
4. E. Schöll, L. Hanschke, L. Schweickert, *et al.*, “Resonance Fluorescence of GaAs Quantum Dots with Near-Unity Photon Indistinguishability”, *Nano Lett.* **19**, 2404 (2019).
5. M. Metcalfe, S. M. Carr, A. Muller, *et al.*, “Resolved Sideband Emission of InAs/GaAs Quantum Dots Strained by Surface Acoustic Waves”, *Phys. Rev. Lett.* **105**, 037401 (2010).
6. B. Villa, A. J. Bennett, D. J. P. Ellis, *et al.*, “Surface acoustic wave modulation of a coherently driven quantum dot in a pillar microcavity”, *Appl. Phys. Lett.* **111**, 011103 (2017).
7. M. O. Scully and M. S. Zubairy, *Quantum Optics* (Cambridge University Press, 1997).
8. T. Hahn, D. Groll, H. J. Krenner, *et al.*, “Photon scattering from a quantum acoustically modulated two-level system”, *AVS Quantum Sci.* **4**, 011403 (2022).
9. D. Groll, F. Paschen, P. Machnikowski, *et al.*, “How to Read Out the Phonon Number Statistics via Resonance Fluorescence Spectroscopy of a Single-Photon Emitter”, *Adv. Quantum Technol.* **n/a**, 2300153 (2023).
10. M. Weiß, D. Wigger, M. Nägele, *et al.*, “Optomechanical wave mixing by a single quantum dot”, *Optica* **8**, 291 (2021).
11. D. Wigger, M. Weiß, M. Lienhart, *et al.*, “Resonance-fluorescence spectral dynamics of an acoustically modulated quantum dot”, *Phys. Rev. Res.* **3**, 033197 (2021).
12. J.-W. Pan, Z.-B. Chen, C.-Y. Lu, *et al.*, “Multiphoton entanglement and interferometry”, *Rev. Mod. Phys.* **84**, 777 (2012).
13. H.-H. Lu, M. Liscidini, A. L. Gaeta, *et al.*, “Frequency-bin photonic quantum information”, *Optica* **10**, 1655 (2023).

14. N. Lo Piparo, W. J. Munro, and K. Nemoto, "Quantum multiplexing", *Phys. Rev. A* **99**, 022337 (2019).
15. K. Stannigel, P. Rabl, A. S. Sørensen, *et al.*, "Optomechanical Transducers for Long-Distance Quantum Communication", *Phys. Rev. Lett.* **105**, 220501 (2010).
16. M. Weiß and H. J. Krenner, "Interfacing quantum emitters with propagating surface acoustic waves", *J. Phys. D: Appl. Phys.* **51**, 373001 (2018).
17. P. Delsing, A. N. Cleland, M. J. A. Schuetz, *et al.*, "The 2019 surface acoustic waves roadmap", *J. Phys. D: Appl. Phys.* **52**, 353001 (2019).
18. B. Freeman, J. Schoenfield, and H. Jiang, "Comparison of low frequency charge noise in identically patterned Si/SiO₂ and Si/SiGe quantum dots", *Appl. Phys. Lett.* **108**, 253108 (2016).
19. A. V. Kuhlmann, J. Houel, A. Ludwig, *et al.*, "Charge noise and spin noise in a semiconductor quantum device", *Nat. Phys.* **9**, 570 (2013).
20. R. A. Bogaczewicz and P. Machnikowski, "Resonance fluorescence of noisy systems", *New J. Phys.* **25**, 093057 (2023).

Fidelity of the acoustic control of single photon scattering with semiconductor quantum dots: supplemental document

This is the supplementary material for the article [Link].

CONTENTS

1 Autocorrelation function	1
2 Noise function for white noise	2
3 Autocorrelation function: inelastic part	3
4 Explicit form of the resonance fluorescence spectrum	3
5 Two-tone and single-tone modulation; asymptotics in the strong-noise limit	4
6 Acoustic phase information in the scattering spectrum	4

1. AUTOCORRELATION FUNCTION

In this section we summarize the derivation of the correlation function given by Eq. (2) of the main text.

The Hamiltonian of the system (in the rotating frame and using rotating wave approximation) reads

$$H(t) = \hbar [\omega_0(t) - \omega_L] |1\rangle\langle 1| - \frac{\hbar\Omega}{2} (\sigma_+ + \sigma_-),$$

where Ω is the optical Rabi frequency and $\sigma_+ = \sigma_-^\dagger = |1\rangle\langle 0|$. The system undergoes spontaneous emission with the rate γ , described by the Lindblad superoperator

$$L[\rho] = \gamma \left(\sigma_- \rho \sigma_+ - \frac{1}{2} \{ \sigma_+ \sigma_-, \rho \} \right),$$

where ρ is the density matrix and $\{, \}$ denotes the anticommutator. The Master Equation governing the evolution of the system has the form

$$\frac{d\rho(t)}{dt} = -\frac{i}{\hbar} [H(t), \rho(t)] + L[\rho(t)]. \quad (\text{S1})$$

Denote the solution of Eq. (S1) by $\rho(t) = \mathfrak{L}_{t_0, t}[\rho(t_0)]$. The Lax quantum regression theorem then yields the autocorrelation function in the form

$$G(t_1, t_2) = \text{Tr}(\sigma_- \mathfrak{L}_{t_1, t_2}[\mathfrak{L}_{t_0, t_1}[\bar{\rho}(t_0)] \sigma_+]). \quad (\text{S2})$$

Here t_0 is the initial moment of evolution, while $t_1 - t_0$ is a sufficiently long time for the system to reach its steady state. We find the evolution to the leading order in the Rabi frequency Ω iteratively, following Refs. [1, 2]. Eq. S1 yields the equations of motion for the elements ρ_{01} , ρ_{10} , ρ_{11} of the density matrix in the form $\dot{\rho}_{jl} = a_{jl}\rho_{jl} + i\Omega \sum_{mn} b_{jl, mn} \rho_{mn}$, where $a_{11} = -\gamma$, $a_{01} = a_{10}^* = i\Delta - \gamma/2$, and $b_{11,10} = -b_{11,01} = b_{10,11} = -b_{01,11} = 1/2$. The same holds for an arbitrary matrix, not necessarily a density matrix. Since Eq. (S1) is trace-preserving, one has $\rho_{00} = c_0 - \rho_{11}$, where c_0 is a constant determined by the initial values ($c_0 = 1$ for a density matrix). In the absence of the laser field ($\Omega = 0$) the equation of motion can be solved trivially to yield the zeroth-order propagation

$$\rho_{jl}^{(0)}(t) = \left[\mathfrak{L}_{t_0, t}^{(0)} \rho(t_0) \right]_{jl} = e^{\int_{t_0}^t ds a_{jl}(s)} \rho_{jl}(t_0).$$

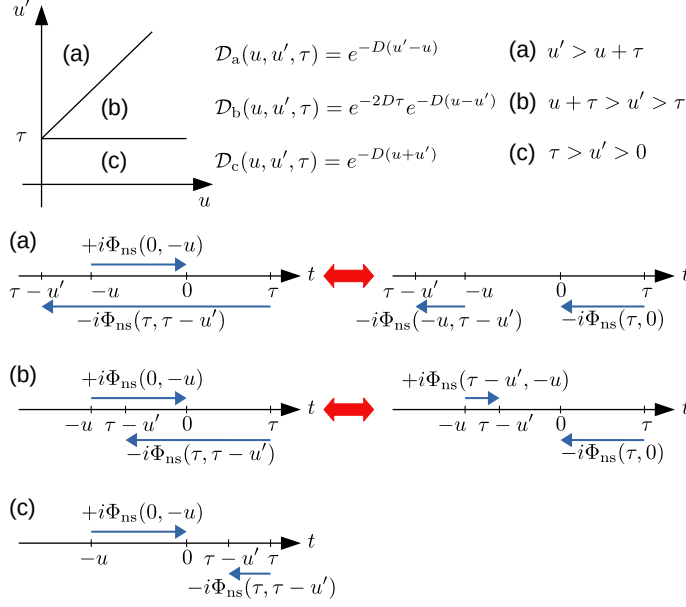


Fig. S1. Upper: division of the (u, u') plane into areas for the calculation of the noise kernel. Lower: Graphical representation of the reduction of the phase evolution intervals into non-overlapping parts.

In the subsequent orders $r > 0$ in Ω ,

$$\rho_{jl}^{(r)}(t) = \left[\mathfrak{L}_{t_0, t}^{(r)} \rho(t_0) \right]_{jl} = i\Omega \int_{t_0}^t ds e^{\int_s^t ds' a_{jl}(s')} \sum_{mn} b_{jl, mn} \rho_{mn}^{(r-1)}(s).$$

These equations define the perturbative expansion of the evolution superoperator \mathfrak{L}_{t_1, t_2} in powers of Ω . Substituting this evolution into Eq. (S2) one finds, in the leading order of Ω^2 , the autocorrelation function in the form [1]

$$G(t_1, t_2) = \frac{\Omega^2}{4} \int_0^\infty du e^{-\frac{\gamma}{2}u} e^{-i\Phi(t_1, t_1 - u)} \int_0^\infty du' e^{-\frac{\gamma}{2}u'} e^{i\Phi(t_2, t_2 - u')}, \quad (\text{S3})$$

where

$$\Phi(t_b, t_a) = \int_{t_a}^{t_b} ds [\omega_L - \omega_0(s)] = \bar{\Delta}(t_b - t_a) - \Phi_{\text{ac}}(t_b, t_a) - \Phi_{\text{ns}}(t_b, t_a). \quad (\text{S4})$$

Here

$$\Phi_{\text{ac}}(t_b, t_a) = \int_{t_a}^{t_b} ds \Delta\omega_{\text{ac}}(s), \quad \Phi_{\text{ns}}(t_b, t_a) = \int_{t_a}^{t_b} ds \Delta\omega_{\text{ns}}(s),$$

we changed the variables according to $s = t + u$ and set $t - t_0 \rightarrow \infty$ (steady-state regime). Substituting the decomposition given by the rightmost form of Eq. (S4) to Eq. (S3) one arrives at Eq. (3) from the main text upon using the fact that the noise is stationary, hence

$$\overline{e^{i\Phi(t_d+s, t_c+s)} \pm i\Phi(t_b+s, t_a+s)} = \overline{e^{i\Phi(t_d, t_c)} \pm i\Phi(t_b, t_a)}.$$

2. NOISE FUNCTION FOR WHITE NOISE

Here we outline the calculations leading to the noise kernel $\mathcal{D}(u, u', \tau)$ in the form of Eq. (4) and Eq. (5) of the main text.

To evaluate the noise kernel given by Eq. (3) of the main text in the case of white noise (phase diffusion), we need to split the two phases Φ_{nc} accumulated over the time intervals $(-u, 0)$ and $(\tau - u', \tau)$ into non-overlapping time intervals that will allow factorization based on the independence of the corresponding increments of the diffusion process. This is done in different ways in each of the areas (a)–(c) in the (u, u') plane shown in the upper part of Fig. S1. We denote

the characteristic functions of these areas by $\Theta_i(u, u'; \tau)$, $i = a, b, c$. In each of the areas, the phases partly cancel in a particular way, which we represent graphically in the lower part of Fig. S1. Here the positive phase is represented by a right-heading arrow above the time axis and the negative phase is shown as a left-heading arrow below, so that each arrow represents an integral of $\Delta\omega_{\text{ns}}$ over the interval from its tail to head. The original phases are shown on the left, while the final form after partial cancellation is on the right. For instance, in area (a), the noise kernel has the form

$$\mathcal{D}_a(u, u', \tau) = \overline{e^{-i\Phi_{\text{ns}}(-u, \tau - u')}} \overline{e^{-i\Phi_{\text{ns}}(\tau, 0)}}.$$

The phase $\Phi_{\text{ns}}(t, t')$ undergoes normal diffusion from time t' to t induced by the white noise $\Delta\omega_{\text{ns}}$ and is therefore normally distributed with zero mean and variance $2D(t - t')$. Therefore

$$\overline{e^{i\Phi_{\text{ns}}(t, t')}} = e^{-D(t-t')},$$

which leads to

$$\mathcal{D}(u, u', \tau) = \mathcal{D}_a(u, u', \tau)\Theta_a(u, u', \tau) + \mathcal{D}_b(u, u', \tau)\Theta_b(u, u', \tau) + \mathcal{D}_c(u, u', \tau)\Theta_c(u, u', \tau)$$

with

$$\mathcal{D}_a(u, u', \tau) = e^{-D(u'-u)}, \quad \mathcal{D}_b(u, u', \tau) = e^{-2D\tau}e^{-D(u-u')}, \quad \mathcal{D}_c(u, u', \tau) = e^{-D(u+u')}.$$

From this, we can extract a part that is undamped in τ ,

$$\mathcal{D}_{\text{el}}(u, u', \tau) = \mathcal{D}_c(u, u', \tau) [\Theta_a(u, u', \tau) + \Theta_b(u, u', \tau) + \Theta_c(u, u', \tau)] = \mathcal{D}_c(u, u', \tau)\theta(u)\theta(u'),$$

which is the contribution given by Eq. (4) of the main text. The remaining part

$$\mathcal{D}_{\text{inel}}(u, u', \tau) = [\mathcal{D}_b(u, u', \tau) - \mathcal{D}_c(u, u', \tau)] \Theta_b(u, u', \tau) + [\mathcal{D}_a(u, u', \tau) - \mathcal{D}_c(u, u', \tau)] \Theta_a(u, u', \tau),$$

can be written in the form of Eq. (5) of the main text.

3. AUTOCORRELATION FUNCTION: INELASTIC PART

We present here some details of the derivation of Eq. (9) from the main text of the paper.

Since the phase $\Phi_{\text{ac}}(t, t')$ is defined as a definite integral, one can rearrange the phase factors in Eq. (2) of the main text,

$$\Phi_{\text{ac}}(t_1, t_1 - u) - \Phi_{\text{ac}}(t_2, t_2 - u') = -\Phi_{\text{ac}}(t_2, t_1) + \Phi_{\text{ac}}(t_2 - u', t_1 - u).$$

Next, performing the change of variables $u = (x + y)/2$, $u' = t_2 - t_1 + (x - y)/2$, $-\infty < x < \infty$, $|y| < x < \infty$, and using the expansion from Eq. (6) in the main text, one can write Eq. (2) in the form

$$\begin{aligned} \mathcal{G}_{\text{inel}}(t_1, t_2) &= \frac{\Omega^2}{8} e^{-(\frac{\gamma}{2} + D - i\bar{\Delta})(t_2 - t_1)} e^{-i\Phi_{\text{ac}}(t_2, t_1)} \sum_k e^{ik\omega_{\Lambda} t_1} \int_{-\infty}^{\infty} dy \phi_k(y) e^{-i\bar{\Delta}y} \\ &\quad \times \int_{|y|}^{\infty} dx e^{-\frac{\gamma + ik\omega_{\Lambda}}{2} x} [e^{-D|y|} - e^{-Dx}]. \end{aligned} \quad (\text{S5})$$

Performing trivial integration over x , then employing Eq. (8) for the integration over y and using Eq. (10) one finds the result in the form of Eq. (9) in the main text.

4. EXPLICIT FORM OF THE RESONANCE FLUORESCENCE SPECTRUM

The spectrum follows in a straightforward way from the exponential τ -dependence in Eq. (7). We present the formulas here for completeness.

Substituting $t_1 = t$, $t_2 = t + \tau$ to Eq. (7), integrating over t according to Eq. (13) and then substituting to Eq. (12) immediately yields the elastic part of the spectrum in the form

$$S_{\text{el}}(\omega) = F_0 \text{Re} \sum_n \frac{\Gamma |c_n|^2}{\Gamma - i(\omega - \omega_L - n\omega_{\Lambda})}. \quad (\text{S6})$$

In the same way, using Eq. (9) we get the inelastic contribution to the spectrum,

$$S_{\text{inel}}(\omega) = \frac{F_0}{2} \text{Re} \sum_{n,k} \frac{\Gamma b_n^* b_{n-k} d_k}{\Gamma + \frac{\gamma}{2} + D - i(\omega - \bar{\omega}_0 - n\omega_{\Lambda})}. \quad (\text{S7})$$

5. TWO-TONE AND SINGLE-TONE MODULATION; ASYMPTOTICS IN THE STRONG-NOISE LIMIT

In this section we derive Eqs. (14), (18) and (19) from the main text. Then we explain how the power-law exponents discussed in the final part of Sec. 3A can be derived.

For a two-tone modulation as in Eq. (16) of the main text, we write the phase in the form

$$i\Phi_{\text{ac}}(t - u', t - u) = 2iA \sin \left[\frac{\omega_A(u - u')}{2} \right] \cos \left[\omega_A t - \frac{\omega_A(u + u')}{2} \right] \\ + iB \sin [\omega_A(u - u')] \cos [2\omega_A t - \omega_A(u + u') + \varphi].$$

Using Jacobi-Anger expansion with respect to the cos terms, while treating the sin terms as coefficients, leads to the expansion in Eq. (6) with the functions ϕ_n given by Eq. (19). The expansion in Eq. (10) with the coefficients given by Eq. (18) is obtained by writing the definite integral $\Phi_{\text{ac}}(t_2, t_1)$ as a difference of originals at the final and initial points and directly applying the Jacobi-Anger expansion. The results for a single-tone harmonic modulation are retrieved by setting $B = 0$.

Functions $\phi_n(u)$ can be written in an alternative form. Let us focus on the factor dependent on B in Eq. (19) (the argument is the same for the other factor). The Bessel function can be written in terms of the defining integral

$$J_k(B \sin \omega_A u) = \frac{1}{2\pi} \int_{-\infty}^{\infty} dt e^{ikt} e^{-iB \sin \omega_A u \sin t}.$$

We write $B \sin \omega_A u \sin t = B[\cos(\omega_A u - t) + \cos(\omega_A u + t)]/2$, apply the Jacobi-Anger expansion twice, and perform the resulting trivial integration over t . The result is

$$J_k(B \sin \omega_A u) = i^{-k} \sum_m J_{m+k}(B/2) J_m(B/2) e^{i(2m+k)\omega_A u}.$$

For moderate modulation amplitudes, only a few Bessel functions contribute. All of them oscillate with the same period when B is sufficiently large. Hence, $J_k(B \sin \omega_A u)$ also oscillates in B and so does $\phi_n(u)$. Upon substituting this expression, along with the analogous expression for $J_{n-2k}(2A \sin \omega_A u/2)$, to Eq. (19) and then to Eq. (8), the integration can be performed analytically and one obtains a summation formula that can be evaluated numerically much faster than the original integral.

To obtain the asymptotic behavior of the scattering intensities for the single-tone modulation in the limit of strong noise, as shown in Fig. 2 of the main text and discussed in Sec. 3A, we need to extract the asymptotics of the coefficients c_n and d_n as $D \rightarrow \infty$ (note that b_n does not depend on D). Substituting $\phi_n^{(1)}(u)$ from Eq. (14) to Eq. (8) and changing the variable to $x = uD$ we obtain

$$c_n^{(1)} = \frac{\gamma^n}{2D} \int_0^\infty dx e^{-\frac{\gamma+2D}{2D}x} e^{-i\frac{\bar{\Delta}+n\omega_A/2}{D}x} J_n \left[2A \sin \left(\frac{\omega_A}{2D} x \right) \right] \approx \frac{\gamma^n}{2D} \int_0^\infty dx e^{-x} J_n \left(\frac{A\omega_A}{D} x \right),$$

where we assumed $D \gg \gamma, \omega_A, \bar{\Delta}$ in the final expression. Substituting the leading term for the Jacobi function, $J_n(z) \approx z^n / (2^n n!)$, $z \ll 1$, we get

$$c_n^{(1)} \approx \frac{\gamma}{2D} \left(\frac{iA\omega_A}{2D} \right)^n \sim D^{-(n+1)}.$$

Then, from Eq. (11), also $d_n \sim D^{-(n+1)}$.

6. ACOUSTIC PHASE INFORMATION IN THE SCATTERING SPECTRUM

We want to develop a quantitative measure of the degree of control of light scattering by the relative phase between two harmonic components of acoustic modulation. Scattering is efficiently controlled by this acoustic phase if the scattering intensity depends on the phase setting, which means that the phase information is encoded in the scattering spectrum. We therefore propose to quantify the fidelity of control in terms of a single-shot attempt to determine the acoustic phase from the accumulated scattering data. We choose the simplest scheme in which the detector is spectrally tuned to the first spectral sideband and the phase is randomly set with equal probabilities to one of the values φ_1 or φ_2 , corresponding, respectively, to the maximum and minimum of the scattering intensity at this spectral position (see Fig. 3 of the main text). Roughly

speaking, the scattering is controlled by the acoustic phase if the detection counts accumulated over a certain period of time allow one to determine whether the scattering intensity is “high” or “low” and thus correctly infer the initial setting of the phase with a high probability. More precisely, the signal is integrated over a period of time T and one opts for φ_1 if the number of counts N is above a threshold value ν . The probability of wrong inference is then given by

$$P_e = p(N \leq \nu | \varphi = \varphi_1) p(\varphi = \varphi_1) + p(N > \nu | \varphi = \varphi_2) p(\varphi = \varphi_2) \quad (\text{S8})$$

$$= \frac{1}{2} [p(N < \nu | \varphi = \varphi_1) + p(N > \nu | \varphi = \varphi_2)].$$

The fidelity of phase control is defined as the probability of correctly determining the phase for an optimal choice of ν .

$$F = \sup_{\nu} (1 - P_e).$$

For the sake of our discussion it is convenient to treat the measurement time as a parameter over which the procedure needs to be optimized in the final step.

With absolutely stable acoustic phase, $p(N = n | \varphi = \varphi_i)$, $i = 1, 2$, are given by Poisson distribution with the distribution parameter (mean count number) $\lambda_i(T) = w_i T$, where w_i are the scattering rates for the two phase settings, proportional to the scattering intensities $I_1 = I_{\max}$ and $I_2 = I_{\min}$. With phase instability, the phase diffuses so that at a time t it is distributed according to the probability density $f_i(\varphi, t)$, $f_i(\varphi, t = 0) = \delta(\varphi - \varphi_i)$. Here we will assume normal diffusion with the diffusion constant D_φ ,

$$f_i(\varphi, t) = \frac{1}{\sqrt{2\pi D_\varphi t}} e^{-\frac{(\varphi - \varphi_i)^2}{2D_\varphi t}}.$$

As a result, while the count distribution remains Poissonian, the scattering rate becomes time-dependent,

$$w_i(t) = \int_{-\infty}^{\infty} d\varphi w(\varphi) f_i(\varphi, t), \quad \lambda_i(T) = \int_0^T d\tau w_i(\tau),$$

where $w(\varphi)$ is the scattering rate for the phase set to φ .

From Eq. (S8) one has

$$P_e = \frac{1}{2} e^{-\lambda_1} \sum_{n=0}^{\lfloor \nu \rfloor} \frac{\lambda_1^n}{n!} + \frac{1}{2} e^{-\lambda_2} \sum_{n=\lfloor \nu \rfloor + 1}^{\infty} \frac{\lambda_2^n}{n!},$$

where $\lfloor \nu \rfloor$ denotes the largest integer not greater than ν . This has a minimum with respect to ν when the two distributions are equal,

$$e^{-\lambda_1} \frac{\lambda_1^n}{n!} = e^{-\lambda_2} \frac{\lambda_2^n}{n!} \text{ for } n = \nu.$$

which yields

$$\nu = 2\lambda\eta \left(\ln \frac{1+\eta}{1-\eta} \right)^{-1}, \quad \lambda = \frac{\lambda_1 + \lambda_2}{2}, \quad \eta = \frac{\lambda_1 - \lambda_2}{\lambda_1 + \lambda_2}.$$

The resulting fidelity is

$$F = \frac{1}{2} + \frac{1}{2} e^{-\lambda} (1 - \eta^2)^{\nu/2} \sum_{n=\lfloor \nu \rfloor + 1}^{\infty} \frac{\lambda^n}{n!} [(1 + \eta)^{n-\nu} - (1 - \eta)^{n-\nu}],$$

which depends on the measurement time via the quantities λ and η .

REFERENCES

1. M. Weiß, D. Wigger, M. Nägele, *et al.*, “Optomechanical wave mixing by a single quantum dot,” *Optica* **8**, 291 (2021).
2. R. A. Bogaczewicz and P. Machnikowski, “Resonance fluorescence of noisy systems,” *New J. Phys.* **25**, 093057 (2023).